

# Evidence of Compton cooling during an X-ray flare supports a neutron star nature of the compact object in 4U1700–37

M. Martínez-Chicharro<sup>1</sup>\* J. M. Torrejón<sup>1</sup> L. Oskinova<sup>2</sup> F. Fürst<sup>3</sup> K. Postnov<sup>4</sup>  
J.J. Rodes-Roca<sup>1</sup> R. Hainich<sup>2</sup> and A. Bodaghee<sup>5</sup>

<sup>1</sup>*Instituto Universitario de Física Aplicada a las Ciencias y las Tecnologías, Universidad de Alicante, 03690 Alicante, Spain*

<sup>2</sup>*Institute for Physics and Astronomy, Universität Potsdam, 14476 Potsdam, Germany*

<sup>3</sup>*European Space Astronomy Centre (ESAC), Science Operations Department, 28692 Villanueva de la Cañada, Madrid, Spain*

<sup>4</sup>*Sternberg Astronomical Institute, Moscow M.V. Lomonosov State University, 119234 Moscow, Russia*

<sup>5</sup>*Dept. of Chemistry, Physics and Astronomy, Georgia College, 221 N. Wilkinson St., Milledgeville, GA 31061, USA*

Accepted XXX. Received YYY; in original form ZZZ

## ABSTRACT

Based on new *Chandra* X-ray telescope data, we present empirical evidence of plasma Compton cooling during a flare in the non pulsating massive X-ray binary 4U1700–37. This behaviour might be explained by quasispherical accretion onto a slowly rotating magnetised neutron star. In quiescence, the neutron star in 4U1700–37 is surrounded by a hot radiatively cooling shell. Its presence is supported by the detection of mHz quasi periodic oscillations likely produced by its convection cells. The high plasma temperature and the relatively low X-ray luminosity observed during the quiescence, point to a small emitting area  $\sim 1$  km, compatible with a hot spot on a NS surface. The sudden transition from a radiative to a significantly more efficient Compton cooling regime triggers an episode of enhanced accretion resulting in a flare. During the flare, the plasma temperature drops quickly. The predicted luminosity for such transitions,  $\sim 3 \times 10^{35}$  erg s<sup>-1</sup>, is very close to the luminosity of 4U1700–37 during quiescence. The transition may be caused by the accretion of a clump in the stellar wind of the donor star. Thus, a magnetised NS nature of the compact object is strongly favoured.

**Key words:** X-rays: binaries – Stars: individual: 4U1700–37 , V\*V884 Sco

## 1 INTRODUCTION

High Mass X-ray Binaries (HMXBs) are fundamental laboratories where the structure of the stellar wind in massive stars as well as the physics of accretion onto compact objects can be studied in detail (Martínez-Núñez et al. 2017, for a recent review). One of the best studied HMXBs in the Galaxy, 4U1700–37, consists of a O6Iafcp donor star (V\*V884 Sco; Sota et al. (2014)) and a compact object on the 3.41 d orbit at an average orbital distance of  $a \approx 1.6R_*$ .

Despite the vast amount of multiwavelength observational data accrued so far, the nature of the compact object in 4U1700–37, remains a mystery. No coherent pulsations have ever been found in X-rays or any other wavelengths. The mass determinations of the compact object give  $2.44 \pm 0.27M_\odot$  (Clark et al. 2002), quite high for a neutron

star<sup>1</sup> (NS), but too low compared with the smallest black hole (BH) found so far. Indirect evidence supporting the presence of a NS has been provided based on the X-ray spectra (Seifina et al. 2016) or the X-ray colour-colour behaviour (Vrtilek & Boroson 2013). A BH, in turn, has been favoured based on timing properties (Dolan 2011).

The donor star in 4U1700–37, V\*V884 Sco, is one of the most massive stars ( $M_* = 58 \pm 11M_\odot$ ) known in the Galaxy and the most massive donor known in any Galactic HMXB. The inner parts of OB-star winds ( $a < 2R_*$ ) are inhomogeneous and clumped (Torrejón et al. 2015) but their properties are not well known. In the past, several studies have used the compact object in 4U1700–37 to probe in situ the donor star wind. Haberl et al. (1989), using *EXOSAT*, studied the radial wind density stratification, via photoelectric absorption. van der Meer et al. (2005) performed a study of

<sup>1</sup> although still below the Tolman-Oppenheimer-Volkoff limit of  $\sim 3 M_\odot$

\* E-mail: maria.chicharro@ua.es

**Table 1.** Observations journal

ObsID	Date	$t_{\text{exp}}$	$\phi_{\text{orb}}$
17630	2015-02-22 03:11:16	14.27	0.13 <sup>a</sup>

<sup>a</sup> Mid eclipse time  $T_0 = 49149.412 \pm 0.006$  MJD, orbital period  $P = 3.411660 \pm 0.000004$  d (Islam & Paul 2016)

the emission lines excited in the stellar wind by the powerful X-ray source, using *XMM-Newton*. Hints of highly ionized iron were detected but could not be completely disentangled from the nearly neutral Fe  $K\alpha$  line at the *EPIC-CCD* resolution. The *XMM-Newton* light curves showed an *off state*, when the X-ray count rate dropped to zero for a short time. van der Meer et al. (2005) attributed this off state to the gap between two successive clumps propagating in the stellar wind.

In this *Letter* we present a 14 ks *Chandra* observation of 4U1700–37 during which the source flared. This enables us to investigate the changes in spectral properties at different luminosities.

The paper is structured as follows: in Section 2 we present the observational details. In sections 3 and 4 we analyse the light curve and time resolved spectra of the source, providing the best fit parameters for the continuum and the Fe emission lines. Finally, in Sections 5 and 6 we discuss these parameters in the framework of the theory and present the conclusions.

## 2 OBSERVATIONS

The DDT observations of 4U1700–37 were performed by *Chandra* on 22 Feb. 2015, simultaneously with the *Hubble Space Telescope* (*HST*, P.I. L. Oskinova)<sup>2</sup>. The High Energy Transmission Gratings spectrometer on-board of *Chandra* (HETG; Canizares et al. (2005)) acquired data during a total of 14.27 ks. The HETG provides spectra with two sets of gratings, the High Energy Grating (HEG) which offers a resolution of 0.011 Å in the bandpass of about 1.5 to 16 Å, and the Medium Energy Grating (MEG) which offers a resolution of 0.021 Å in the bandpass of about 1.8 to 31 Å. The spectra were reduced using standard procedures with the CIAO software (v 4.4) and the response files were generated (**arf** and **rmf**). First dispersion orders ( $m = \pm 1$ ) were extracted and analysed simultaneously. The peak source flux both at HEG and MEG gratings is  $4.4 \text{ s}^{-1}$ , which is much lower than the level at which pileup starts to be important<sup>3</sup>. The spectral analysis was performed with the Interactive Spectral Interpretation System (ISIS) v 1.6.1-24 (Houck & Denicola 2000).

<sup>2</sup> The *HST* UV observations will be reported in the follow up publication, Hainich et al. in prep.

<sup>3</sup> See *The Chandra ABC Guide to Pileup*, v.2.2, <http://cxc.harvard.edu/ciao/download/doc/pileup-abc.pdf>

## 3 LIGHT CURVES AND TIMING

Figure 1 shows the extracted light curves in the hard 1.5 - 4 Å (H) and soft 4 - 15 Å (S) bands. Both light curves are strongly variable as typical in wind accreting HMXBs. Two episodes are remarkable. The most obvious one lasts from  $\sim 7600$  s to 13000 s when the source undergoes a flare after which it returns to the quiescence brightness levels. The hardness ratio,  $\text{HR} = \text{H-S}/\text{H+S}$ , does not show any noticeable change, even during the flare. The second episode is the period of very-low flux, between 7200 s and 7350 s, preceding the flare. During the low flux period, the count-rate in the soft band is consistent with zero counts. Similar *off-states* are often observed in systems containing magnetised NS (eg. Vela X-1; Kreykenbohm et al. (2008)). To our knowledge, the off-states have not been observed in HMXBs that contain a black hole.

In the right panel of Fig. 1 we show the standard Lomb-Scargle periodogram of *Chandra* HETG 1.5-10 Å light curve, binned to 5 s, separately for the quiescence and flare. In agreement with previous observations, we do not see any signatures of coherent pulsations. However, the periodogram clearly shows several mHz quasi periodic oscillations (QPOs) more noticeable during the flare. The false alarm probability of the  $0.63 \pm 0.05$  mHz peak is lower than 1%. Such QPOs at mHz frequencies have already been reported for 4U1700–37 on the basis of *Chandra* (Borison et al. 2003) and *RXTE* observations (Dolan 2011).

## 4 SPECTRA

### 4.1 Continuum modeling

In order to shed light on the mechanism that triggered the flare, we want to trace plasma changes by performing time resolved spectroscopy during the time intervals  $t = [0-7600, 13000-14200]$  s (quiescence) and  $t = [7600-13000]$  s (flare). We successfully fit the continuum with the bulk motion comptonisation model (BMC) (Titarchuk et al. 1997). BMC is a general model for comptonisation of soft photons which uses the Green's (spread) functions for the treatment of upscattering and which attains the form of a broken powerlaw. This formalism is valid for any kind of comptonisation (bulk comptonisation in first order ( $v/c$ ), thermal comptonisation in second order ( $v/c$ )<sup>2</sup>) and remains valid up to photon energies comparable to the mean plasma energy ( $m_e c^2 \sim 511$  keV in the case of bulk motion). In the case of a BH, the soft component originates in the innermost part of the accretion disk where the gravitational energy of matter is released due to viscous dissipation and geometric compression. In the case of a NS the soft component is likely produced by a hot spot on the NS surface. Either the disk or the surface (or both) emit a soft black body like spectrum with a characteristic colour temperature  $kT_{\text{col}}$ . The comptonizing region (a cloud or a boundary layer) must cover effectively this zone (i.e. the innermost region of the disk or the spot over the surface) in order to be well exposed to a high fraction of the seed photons. Parameter  $f$  describes the ratio of the number of photons multiply-scattered in the converging inflow to the number of photons in the thermal component. During fitting procedure we have fixed it at 10

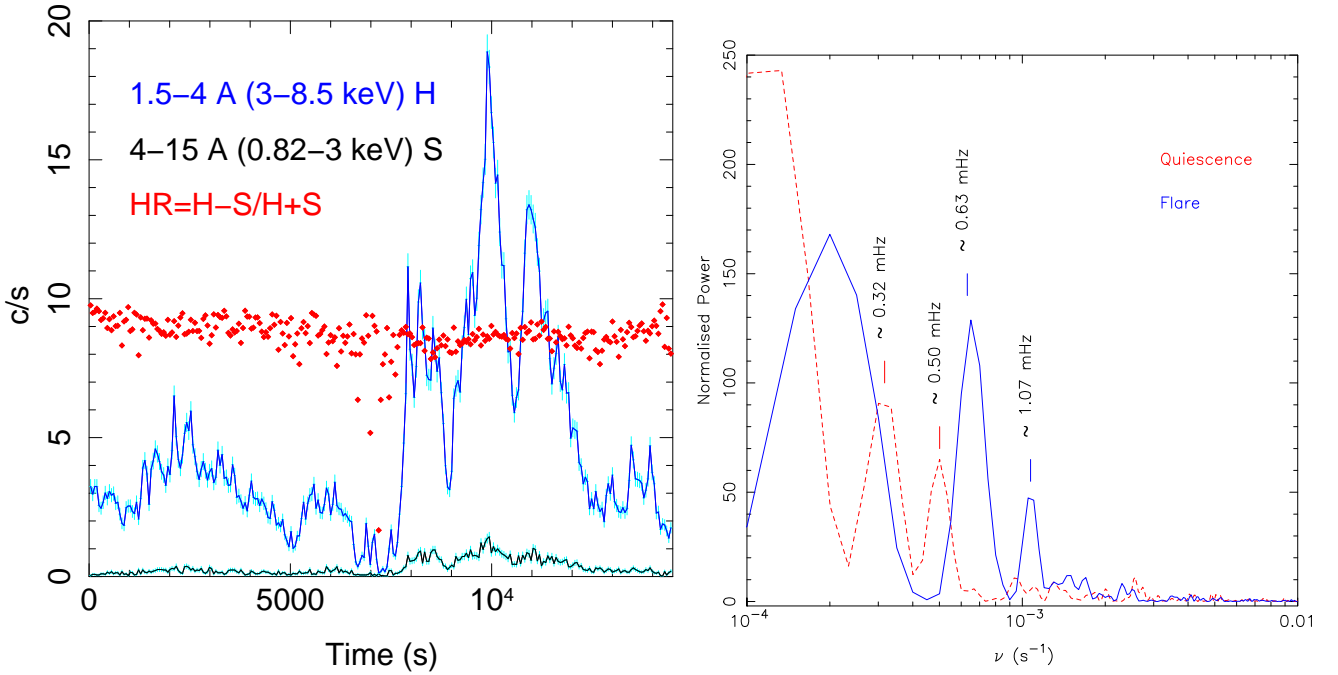


**Figure 1.** *Chandra* HETG lightcurve, in the 1.2 - 15 Å wavelength range, grouped in 10 s bins. The HR seems to be constant even during the flare. Right panel: Lomb-Scargle periodogram of the *Chandra* HETG lightcurve binned to 5s for quiescence and flare. No coherent period is found but a number of ~ mHz QPOs are detected, most prominently during the flare.

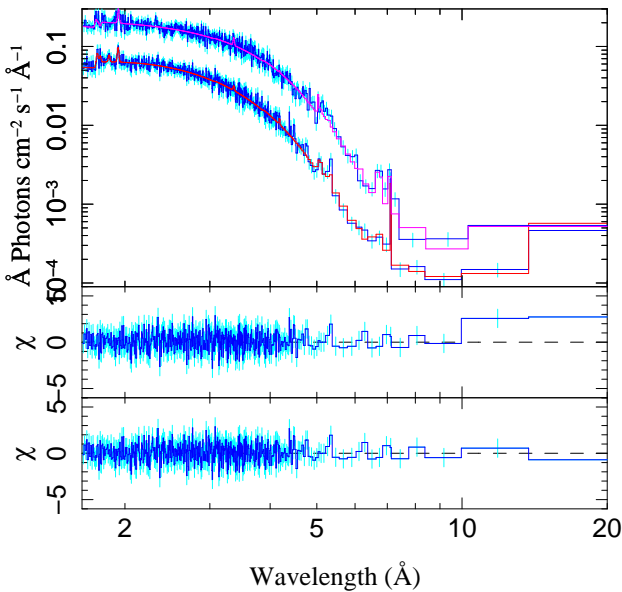


**Figure 2.** *Chandra* HETG spectra during quiescence and flare grouped in  $5\sigma$  bins. Residuals are shown for the BMC model (mid panel) during quiescence (residuals during flare are similar). The soft excess seen at long wavelengths, found in the spectra of many HMXBs (Hickox et al. 2004), can be described by the addition of a blackbody with  $N_{H,3}$  ( $10^{22}$  cm $^{-2}$ ) =  $0.3 \pm 0.1$  and  $kT_{bb} = 0.095^{+0.007}_{-0.011}$  keV (bottom panel). This component, however, is marginal and its addition here does not improve the fit.

( $\gg 1$ ) meaning that the Compton cloud efficiently covers the soft photons source<sup>4</sup>.

One of the three free parameters of the BMC model is a power law spectral index  $\alpha$  describing the Comptonisation efficiency. When  $\alpha$  is smaller the spectrum is harder due to enhanced efficiency (for details see Sunyaev & Titarchuk (1980)). On the contrary, larger  $\alpha$  describes softer spectra. A value close to unity indicates that the source is undergoing a phase transition from the low-hard to a high-soft state. The transitions can be caused by a number of mechanisms, e.g. the redistribution of mass accretion rates between Keplerian disk and sub-Keplerian components in a disk or by an increase of the optical depth  $\tau_0$  for gravitational energy release at the shock (BH case) or at the surface (NS case).

The emitted X-ray continuum described above must be modified at low energies by photoelectric absorption  $ABS(E)$  in order to account for the local and interstellar absorption effects. The observed continuum is thus  $F(E) = ABS(E) \times BMC(E)$  where the absorber is described by

$$Abs(E) = \left( \epsilon \times e^{-\sigma(E)N_{H,1}} + (1 - \epsilon) \times e^{-\sigma(E)N_{H,2}} \right) \quad (1)$$

Here  $\epsilon$  is the covering fraction which acts as a proxy for the massive star wind clumping. The photoelectric absorption has been modelled using `tbnew` which contains the most up to date cross sections for X-ray absorption<sup>5</sup>. The best fit parameters are presented in Table 2.

<sup>4</sup> Given the limited energy range covered by *Chandra*, the model is not sensitive to the exact value of  $f$

<sup>5</sup> <http://pulsar.sternwarte.uni-erlangen.de/wilms/research/tbabs/index.html>

**Table 2.** Model BMC continuum parameters.

Parameter	Quiescence	Flare
BMC		
$N_{\text{H},1}$ ( $10^{22}$ cm $^{-2}$ )	$18.9^{+0.2}_{-0.2}$	$19.36^{+0.19}_{-0.19}$
$\epsilon$	$0.995^{+0.001}_{-0.001}$	$0.994^{+0.001}_{-0.001}$
$N_{\text{H},2}$ ( $10^{22}$ cm $^{-2}$ )	$0.30^{+0.30}_{-0.20}$	$2.53^{+0.36}_{-0.30}$
Norm	$0.0142^{+0.0001}_{-0.0001}$	$0.0627^{+0.0006}_{-0.0006}$
$kT_{\text{col}}$ (keV)	$1.43^{+0.01}_{-0.01}$	$0.58^{+0.01}_{-0.01}$
$\alpha$	$1.25^{+0.04}_{-0.03}$	$0.186^{+0.003}_{-0.003}$
$f$	10 (fixed)	10 (fixed)
Flux <sup>a</sup>	$8.00^{+0.05}_{-0.05}$	$45.00^{+0.27}_{-0.27}$
$\chi^2_{\text{r}}(\text{d.o.f.})$	0.96(443)	0.98(467)

<sup>a</sup> Unabsorbed 1.5 – 20 Å flux,  $\times 10^{-10}$  erg s $^{-1}$  cm $^{-2}$

During quiescence, the column density  $N_{\text{H},2} = N_{\text{H}}^{\text{ISM}} = 0.30^{+0.28}_{-0.23} \times 10^{22}$  cm $^{-2}$  is compatible with the interstellar medium (ISM) absorption towards V\*V884 Sco, deduced from the optical extinction,  $E(B - V) = 0.54 \pm 0.02$  (Clark et al. 2002) and using the relationship  $N_{\text{H}} = 6.12 \times 10^{21} E(B - V)$  (Gudennavar et al. 2012). On the other hand,  $N_{\text{H},1}$  is much larger during the flare, consistent with the thick stellar wind expected in a O6.5 supergiant star.

The spectral powerlaw index  $\alpha$  goes from  $\sim 1.2$  during quiescence to  $\sim 0.19$  during the flare showing that the comptonisation is more efficient when the luminosity (presumably the mass accretion rate) increases. At the same time, the soft photon source temperature  $kT_{\text{col}}$  decreases from 1.43 keV ( $\sim 16$  MK) to 0.58 keV (7 MK) during the flare when the comptonisation (hence the Compton cooling) is more efficient. Thus we observe plasma that cooled down by about 9 million degrees on the time scale of an hour.

## 4.2 Fe lines

The plasma cooling during the flare due to enhanced Compton efficiency is strongly supported by the analysis of the highly ionised iron lines. Figure 3 shows the Fe  $K\alpha$  line region during quiescence and flare. The quiescence spectra (left panel) show lines from the low ionised Fe ( $K\alpha$  and  $K\beta$  fluorescence, along with the Fe K edge at 1.7 keV) as well as from highly ionised states (Fe XXV He like and Fe XXVI H-like Ly  $\alpha$ ). These transitions arise in the circum-source material illuminated by the powerful source of X-rays from the accretion onto the compact object. In order to measure line fluxes we fitted them as gaussians. Table 3 lists corresponding best fit parameters.

During the flare the  $K\alpha$  fluorescence line from nearly neutral Fe remain largely unaffected. The line flux increase in response to the increased illumination (higher X-ray continuum) but the equivalent width ( $EW$ ) stays constant (see Table 3). In contrast, the highly ionised species (He like Fe XXV and H like Fe XXVI Ly  $\alpha$ ), disappear. These lines are produced in very high temperature plasma. During the episode of enhanced cooling, the Fe ionisation drops and these lines

should become less prominent. This is indeed confirmed by observations. On the other hand, the transition of H like Fe XXVI Ly  $\alpha$  seems to appear in absorption during the flare, hinting to the presence of a warm absorber, although the large associated errors prevent a firm conclusion. At any rate, the highly ionised Fe lines decrease significantly (or vanish) during the flare.

## 5 DISCUSSION

The phenomenology presented above can be readily explained as an episode of Compton plasma cooling during a flare. This behaviour is predicted in accreting NS systems with moderate X-ray luminosities, undergoing quasi spherical subsonic accretion (Shakura et al. 2012).

At a distance of  $d \simeq 2$  kpc (Ankay et al. 2001; Megier et al. 2009), the (un absorbed) luminosity of 4U1700–37, is  $L_X \approx 4 \times 10^{35}$  erg s $^{-1}$  during quiescence. At such luminosities, direct (Bondi) wind accretion is hampered by the need of the plasma to cool. If  $t_{\text{cool}} \gg t_{\text{freefall}}$  the matter undergoes subsonic settling accretion and a quasi spherical shell appears around the NS between the magnetospheric radius and the Bondi radius. The presence of a convective shell is supported by the presence of mHz QPOs in the light curve. These QPOs might reflect the convective motions inside the shell.

On the other hand, the luminosity of 4U1700–37 in quiescence is very close to the threshold predicted for a phase transition from radiative to Compton cooling,  $\sim 3 \times 10^{35}$  erg s $^{-1}$  (Shakura et al. 2013). Hence, 4U1700–37 is very prone to such transitions which may easily be caused by a local perturbation in the accretion flow. Following the transition, the enhanced efficiency of the Compton cooling further increases the ability of matter to enter the magnetosphere and accrete. This runaway process leads to a flare. During the observed flare, the luminosity reached  $L_X \approx 2 \times 10^{36}$  erg s $^{-1}$ , still too low for the direct Bondi accretion regime.

In our observation, the flare is preceded by an off-state (see Fig. 1). As a possible explanation for these observational facts, one may consider a clumped stellar wind, where the medium between clumps is strongly rarefied (Oskinova et al. 2012). In this case, a perturbation caused by the ingestion of a wind clump (flare) would be preceded by a short period of time when the wind in the vicinity of the NS is void (off-state).

At the quasi-spherical settling accretion stage, the neutron star equilibrium spin period can be very long, about thousand seconds for the canonical neutron star magnetic field  $10^{12}$  G and typical stellar wind velocities of about 1000 km s $^{-1}$  (Shakura et al. 2012). The spin period is almost directly proportional to the NS magnetic field, and for a highly magnetised NS can be a few ten thousand seconds or even longer (Sidoli et al. 2017, 36.2 ks in AX J1910.7+091). This may explain the non-detection of coherent pulsations.

Despite the lack of pulse detection, other pieces of evidence support the presence of a magnetised NS. The temperature of the soft photons is rather high during quiescence. To reconcile the high colour temperature of the soft emitting region  $T_{\text{col}} \sim 1.4$  keV with the low intrinsic luminosity ( $L_X \sim 10^{35}$  erg s $^{-1}$ ) a small emission area must be invoked. Assuming that the source is radiating as a black

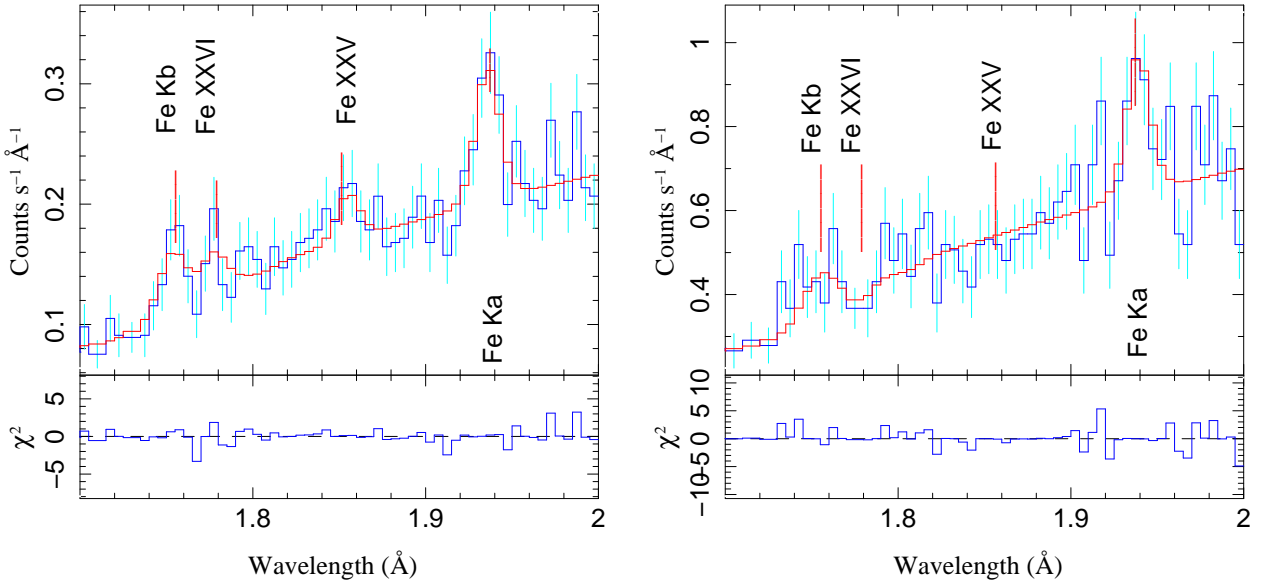


**Figure 3.** *Chandra* HETG spectra and the best fit model, in the 1.6 – 2.1 Å range, during quiescence (left) and flare (right) respectively. The lower panels show the quality of fit.

**Table 3.** Fe lines parameters. Numbers without errors have been fixed at the quoted values.

Ion	Quiescence				Flare			
	$\lambda$ (Å)	Flux $\times 10^{-6}$ (ph s $^{-1}$ cm $^{-2}$ )	$\sigma$ (Å)	$EW$ (mÅ)	$\lambda$ (Å)	Flux $\times 10^{-6}$ (ph s $^{-1}$ cm $^{-2}$ )	$\sigma$ (Å)	$EW$ (mÅ)
Fe K $\beta$	1.753 $^{+0.003}_{-0.004}$	190 $^{+180}_{-90}$	0.005	21 $^{+6}_{-6}$	1.756 $^{+0.052}_{-0.052}$	251 $^{+400}_{-150}$	0.005	8 $^{+1}_{-7}$
Fe xxvi Ly $\alpha$	1.777 $^{+0.002}_{-0.006}$	125 $^{+80}_{-125}$	0.005	7 $^{+24}_{-4}$	1.777 $^{+0.002}_{-0.011}$	-240 $^{+290}_{-430}$	0.005	-8 $^{+1}_{-13}$
Fe xxv	1.855 $^{+0.004}_{-0.000}$	170 $^{+100}_{-50}$	0.005	18 $^{+18}_{-1}$	1.855 $^{+0.004}_{-0.004}$	0.00 $^{+192}_{-0.01}$	0.005	0.0 $^{+0.4}_{-0.1}$
Fe K $\alpha$	1.935 $^{+0.003}_{-0.003}$	330 $^{+120}_{-90}$	0.005	33 $^{+11}_{-8}$	1.939 $^{+0.004}_{-0.003}$	970 $^{+30}_{-380}$	0.005	31.3 $^{+0.7}_{-12.2}$

body of area  $4\pi R_W^2$ , the radius of the emitting area would be  $R_W = 0.3\sqrt{L_{34}}(kT_{col}/1\text{keV})^{-2} \simeq 0.9$  km, which is only compatible with a hot spot over the NS surface. On the other hand, during the flare this radius turns out to be much larger, of the order of 12 km, comparable in size to the entire NS.

## 6 CONCLUSIONS

We present empirical evidence of plasma Compton cooling during a flare in 4U1700–37. This is supported by the analysis of the X-ray continuum as well as the disappearance of the highly ionised Fe lines. This behaviour can be explained by the sudden accretion of the hot shell that forms around the NS when a transition from a radiative cooling regime to a much more efficient Compton cooling, occurs. The predicted luminosity for such transitions, namely  $\sim 3 \times 10^{35}$  erg s $^{-1}$  (Shakura et al. 2013) is very close to where 4U1700–37 stays during quiescence. The presence of such hot shell is further supported by the detection of mHz QPOs produced by convection cells in the shell. To reconcile the high plasma

temperature with the low  $L_X$  a small emitting area  $R_W \sim 1$  km, must be invoked, only compatible with a hot spot on a NS surface. Therefore, a magnetised NS is strongly favoured by the available data. The lack of coherent pulsations may indicate a very long spin period of a strongly magnetised neutron star with  $B > 10^{13}$  G.

## ACKNOWLEDGEMENTS

This research has been supported by the grant ESP2014-53672-C3-3P. AB acknowledges support from STScI award 44A-1096046. JJRR acknowledges support from MECD fellowship PRX17/00114. This research has made use of the ISIS functions provided by ECAP/Remeis observatory and MIT. We thank *Chandra* director for the approval of the Director’s Discretionary Time observation and the anonymous referee whose comments improved the content of the paper.

## REFERENCES

- Ankay A., Kaper L., de Bruijne J. H. J., Dewi J., Hoogerwerf R., Savonije G. J., 2001, *A&A*, **370**, 170
- Boroson B., Vrtillek S. D., Kallman T., Corcoran M., 2003, *ApJ*, **592**, 516
- Canizares C. R., et al., 2005, *PASP*, **117**, 1144
- Clark J. S., Goodwin S. P., Crowther P. A., Kaper L., Fairbairn M., Langer N., Brocksopp C., 2002, *A&A*, **392**, 909
- Dolan J. F., 2011, preprint, ([arXiv:1107.1537](https://arxiv.org/abs/1107.1537))
- Gudennavar S. B., Bubbly S. G., Preethi K., Murthy J., 2012, *ApJS*, **199**, 8
- Haberl F., White N. E., Kallman T. R., 1989, *ApJ*, **343**, 409
- Hickox R. C., Narayan R., Kallman T. R., 2004, *ApJ*, **614**, 881
- Houck J. C., Denicola L. A., 2000, in Manset N., Veillet C., Crabtree D., eds, *Astronomical Society of the Pacific Conference Series* Vol. 216, *Astronomical Data Analysis Software and Systems IX*. p. 591
- Islam N., Paul B., 2016, *MNRAS*, **461**, 816
- Kreykenbohm I., et al., 2008, *A&A*, **492**, 511
- Martínez-Núñez S., et al., 2017, *Space Sci. Rev.*,
- Megier A., Strobel A., Galazutdinov G. A., Krelowski J., 2009, *A&A*, **507**, 833
- Oskinova L. M., Feldmeier A., Kretschmar P., 2012, *MNRAS*, **421**, 2820
- Seifina E., Titarchuk L., Shaposhnikov N., 2016, *ApJ*, **821**, 23
- Shakura N., Postnov K., Kochetkova A., Hjalmarsdotter L., 2012, *MNRAS*, **420**, 216
- Shakura N., Postnov K., Hjalmarsdotter L., 2013, *MNRAS*, **428**, 670
- Sidoli L., Israel G. L., Esposito P., Rodríguez Castillo G. A., Postnov K., 2017, *MNRAS*, **469**, 3056
- Sota A., Maíz Apellániz J., Morrell N. I., Barbá R. H., Walborn N. R., Gamén R. C., Arias J. I., Alfaro E. J., 2014, *ApJS*, **211**, 10
- Sunyaev R. A., Titarchuk L. G., 1980, *A&A*, **86**, 121
- Titarchuk L., Mastichiadis A., Kylafis N. D., 1997, *ApJ*, **487**, 834
- Torrejón J. M., Schulz N. S., Nowak M. A., Oskinova L., Rodes-Roca J. J., Shenar T., Wilms J., 2015, *ApJ*, **810**, 102
- Vrtillek S. D., Boroson B. S., 2013, *MNRAS*, **428**, 3693
- van der Meer A., Kaper L., di Salvo T., Méndez M., van der Klis M., Barr P., Trams N. R., 2005, *A&A*, **432**, 999

This paper has been typeset from a  $\text{\TeX}/\text{\LaTeX}$  file prepared by the author.